Simulation of Adhesive Bonding of a Fiber-Optic Rayleigh Sensor with Composite Material as Part of the Design of a Monitoring System

Konstantin Shramko[1,*], *Nikolay* Kononov[1], *Kirill* Ibrishev[1] and *Diana* Tinchurina[1]
[1]Moscow Aviation Institute (MAI), Moscow, Russia

Abstract. Using fiber optic sensors in the aviation industry is a relevant and promising technology that can significantly improve the safety and efficiency of air travel. Fiber-optic sensors make it possible to warn of potential breakdowns, detect defects in the structure on time, reliably respond to their presence and give timely feedback during operation, which leads to real-time clarification of the state of the aircraft and the need for it to undergo convenient maintenance [1]. In aviation technology, polymer composite materials (PCM) are significantly increasing, in which fiber optic sensors are easily integrated [2]. Adhesive bonding plays a significant role in the durability of a sensor attached to or embedded in a PCM structure. Modelling the adhesive bond between a fiber optic sensor and a composite material makes it possible to determine the optimal physical and mechanical characteristics of the adhesive to increase the durability of the fiber optic sensor and thereby improve the quality of designing aircraft structures [3]. This paper presents the influence of various physical and mechanical properties of the adhesive on fatigue life to determine the optimal parameters for connecting an optical fiber to a composite panel. The results of computer simulation on the Simcenter software platform are presented, in which stresses, the number of cycles to failure that occur in an adhesive joint under various loads, and the physical and mechanical properties of the adhesive are calculated.

1 Introduction

Due to the widespread use of composite materials in the aviation and aerospace industries, the task of creating an integrated system for continuous monitoring of the state of the structure, capable of detecting damage in critical structural elements, is necessary as part of improving flight safety and more efficient maintenance of aviation equipment [4]. The most promising and dynamically developing non-destructive testing method for constructing such systems are fiber-optic sensors (FOS) [5]. The inherent advantages of FOS include their size, the ability to operate in a wide temperature range, immunity to electromagnetic interference, the ability to multiplex, and fire safety [6].

* Corresponding author: Konstantin_home@mail.ru

An essential aspect of using FOS for monitoring the state of a structure made of polymer composite materials (PCM) is the adhesive connection between FOS and composite products [7]. So, for example, in [8], it is noted that the deformations recorded using FOS need to be more representative of the levels of deformation in a structural element. The optical fiber deformation caused by applying a load to the base material is transmitted through the adhesive layer and protective coating. It is subjected to shear at the boundaries of the materials (Fig. **1**). In other words, part of the energy transferred to the FOS goes into shear deformation, which causes the difference in the readings of the deformation values. Accordingly, this should be kept in mind to assess the actual deformations of the base material.

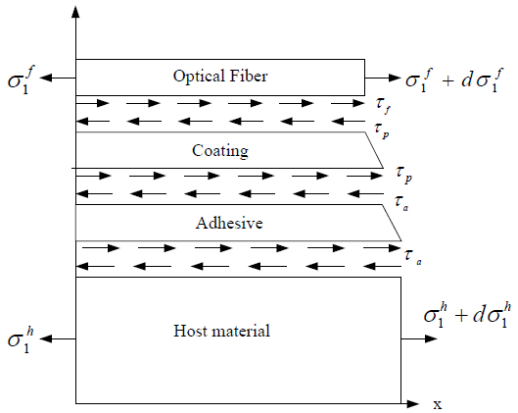

Fig. 1. Analytical model of a FOS attached to a surface.

In this work, the influence of the elastic modulus of the protective coating and the length of the attached FOS on the deformation transfer from the base material to the FOS was studied. As a result of the study, it was concluded that the longer the bonded material and the more complex the coating, the greater the deformation is given to the optical fiber.

In [9], the influence of four geometric parameters of the adhesive layer - the width of the adhesive joint, the upper and lower thickness, and the length of the glued area on the transfer of deformations of the FOS glued to the surface (Fig. **2**) was studied.

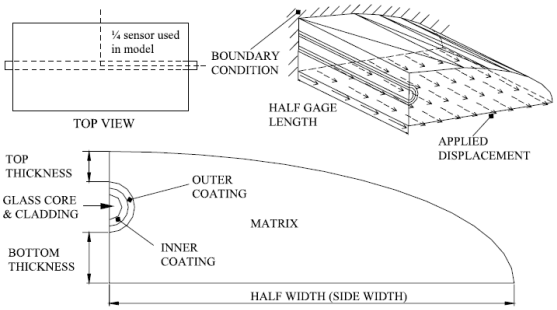

Fig. 2. Adhesive joint parameters.

The authors of this scientific work have identified two critical parameters that affect the completeness of the transfer of deformation. So, for example, at thicknesses of 0.1 mm and 0.5 mm of the adhesive layer between the FOS coating and the base material, the percentage of strain transfer to the FOS was 86% and 73%, respectively. Another important parameter was the length of the glued area of the VOD, which confirms the conclusions of the studies [8].

When analyzing scientific papers on the fatigue life of fiber optic sensors, in [10-11], the influence of the physical and mechanical properties of the protective coating of FOS (acrylate, polyimide, etc.) on the fatigue strength of FOS was studied. Scientific works that directly consider the physical and mechanical characteristics of the adhesive layer (adhesive) are in significant short supply, which determined the topic of this study.

This work aims to study the influence of the physical and mechanical characteristics of the adhesive on the fatigue life of the adhesive joint of a composite panel and a fiber-optic Rayleigh sensor. Different mechanical factors of the bond and the composite panel lead to uneven deformations in the area of their connection under the action of cyclic loads, which in turn leads to delamination and further destruction of the adhesive layer after a certain number of loading cycles. An analysis of the mechanical properties and the suitable adhesive can provide a strong and stable joint with minimal problems in terms of strain compatibility.

2 Model specification

The object of modelling was the zone of an elementary sample from PCM for compression tests according to the ASTM 6641 standard, with a FOS glued to it with an adhesive film.

It is assumed that the simulation of FOS along the entire length of an elementary sample is unwise from the point of view of saving computational power and time. Therefore, in this study, a global-local modeling technique was applied, in which, for a complete assessment of the stress-strain state of the adhesive joint, a detailed local finite element model (FEM) was prepared, including a FOS, a sticky film, and a section of a composite sample. The simulation was carried out in the SimCenter software package using the Samcef solver for static calculations and Specialist Durability - W. Van Papaegem for fatigue life calculations.

In the course of the work, two models were prepared: 1) a global model of a sample made of PCM 140x12 mm, with a symmetrically balanced stacking [45/0/-45/0/90]s, with a sample thickness of 1.8 mm. 2) a local detailed model of the sample zone with a 6x6 mm FOD with identical laying. Finite element models are shown in Fig. **3**.

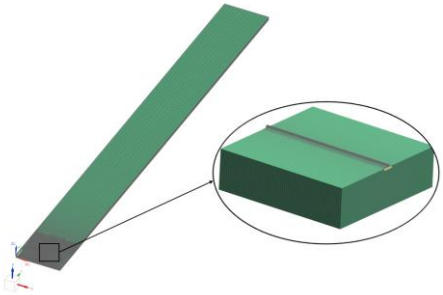

Fig. 3. FEM of global and local models.

3 Global model

A layer-by-layer model of the composite material was adopted, which does not consider each layer's behavior separately, with a glued "Tie" type contact between the layers. The global model is necessary only to remove the resulting displacements obtained from the stress-strain state during sample compression and their further transfer to the local detailed

model. The mechanical properties of the package are given in Table 1. The table contains the following designations:

E1 is Young's modulus along the fibers;
E2 - Young's modulus across the fibers;
G12 is the shear modulus along the layer plane;
ρ is the density of the material;
μ - Poisson's ratio.

Table 1. Package properties from PCM.

E_1, MPa	E_2, MPa	G_{12}, MPa	ρ, kg/m^3	μ
132380	10760	5650	1600	0,24

4 Local model

A layered model of the material was also chosen, in which the nodes of the layers of the package are sewn “knot to knot” since the area of interest is an adhesive joint. In this model, cohesive contact was used between: the surface of the FOS and the sticky film, the adhesive film, and the upper layer of the sample. The criteria for fracture and crack growth were specified for the cohesive contact. The mechanical properties of the adhesive are shown in Table 2.

Table 2. Adhesive properties.

E, MPa	ρ, kg/m^3	μ
3144	1300	0,33

In this work, a Rayleigh-type distributed fiber-optic sensor was chosen as a sensitive element of the structure state monitoring system. The mechanical properties of the fiber optic sensor are shown in Table 3.

Table 3. Properties of the fiber optic sensor.

E, MPa	ρ, kg/m^3	μ
86900	2400	0,29

The FEM of the local model is shown in Fig. **4**.

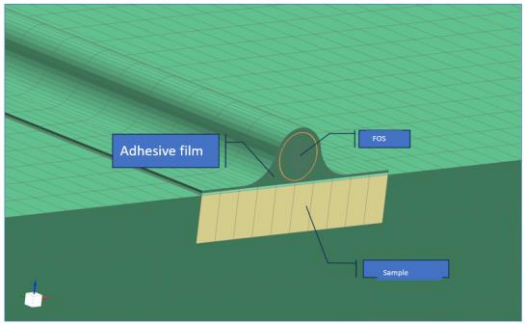

Fig. 4. FEM local model.

To carry out a static calculation of the prepared global model, boundary conditions were used: rigid termination in all degrees of freedom from one end and a compressive load P = 1000 N from the other (Fig. **5**).

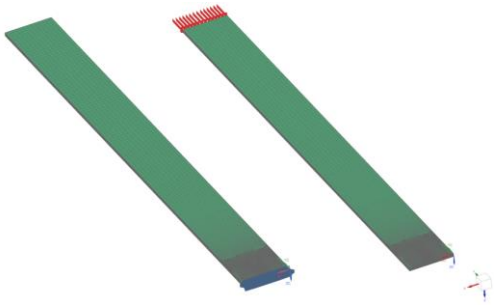

Fig. 5. Boundary conditions for calculating the global model.

5 Simulation results

5.1 Static calculations

A static calculation was carried out according to the described design case of loading a PCM sample. Fig. **6** shows the displacement field due to the action of a compressive load. Figures Fig. **7** – Fig. **8** show the stress-strain state of the sample.

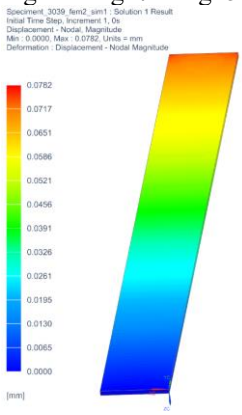

Fig. 6. The displacement field of the global model at P=1000 N, mm.

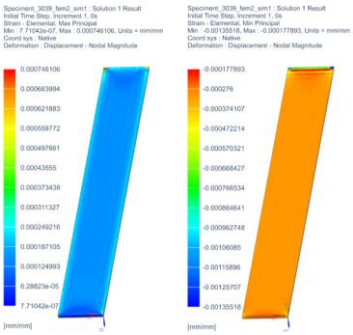

Fig. 7. Maximum and minimum main deformations of the global model, mm/mm.

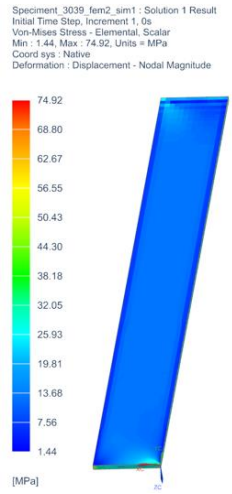

Fig. 8. Average stresses according to von Mises of the global model, MPa.

The field of displacements of the calculation zone for calculations of a detailed local model and the average stresses according to Mises are presented in Figures Fig. **9** – Fig. **12**.

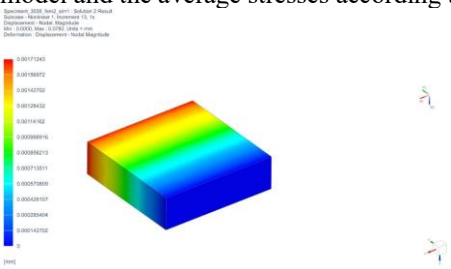

Fig. 9. The displacement field of the computational zone for the local model, mm.

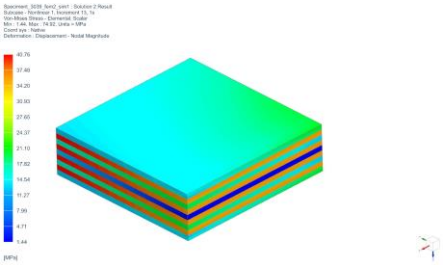

Fig. 10. Average von Mises stresses of the design zone for the local model, MPa.

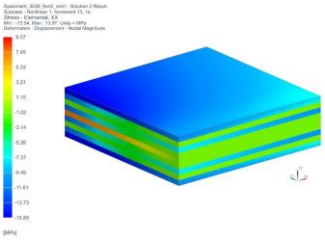

Fig. 11. Principal stresses along the X-axis of the calculation zone for the local model, MPa.

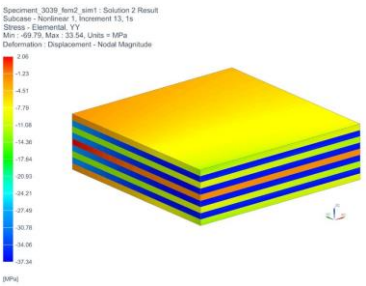

Fig. 12. Principal stresses along the Y-axis of the computational zone for the local model, MPa.

Further, after conducting a static calculation on the global model, using the global-local modeling technique, a fixed estimate of a detailed local model was carried out, which consists of transferring the calculation zone's displacement field. The nodes to which the stress-strain state was transferred are shown in Fig. **13**. The transferred displacement field will be the boundary conditions for calculating the detailed local model.

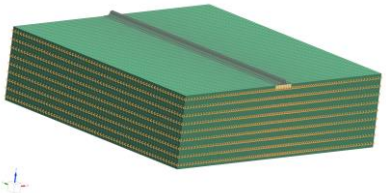

Fig. 13. A set of nodes for transferring VAT from the global model to the local one.

A static calculation of the local FEM of the sample was carried out to verify the correctness of the SSS transfer technique. The calculation results are shown in Figures Fig. **14** – Fig. **17**.

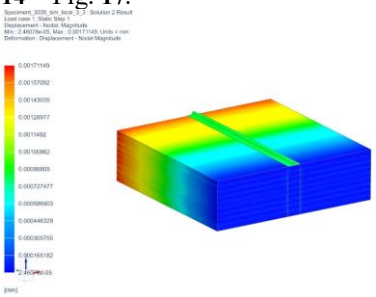

Fig. 14. The displacement field of the local model, mm.

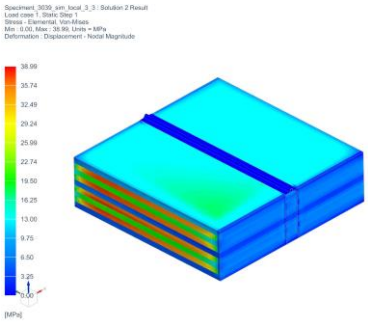

Fig. 15. Average stresses according to von Mises of the local model, MPa.

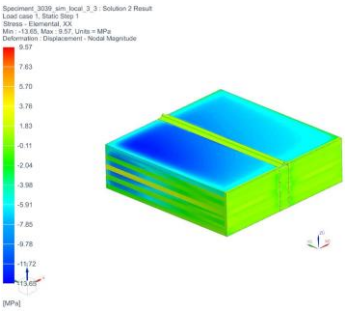

Fig. 16. Principal stresses along the X axis of the local model, MPa.

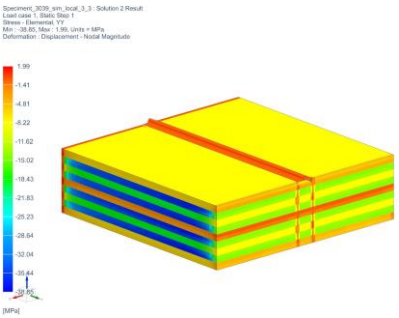

Fig. 17. Principal stresses along the Y axis of the local model, MPa.

According to the calculation results, the global-local modeling technique works correctly. The SSS of the computational zone of the global model was compared with the SSS obtained on the local model in terms of the displacement field, average von Mises stresses, and principal stresses along the X and Y axes of the global coordinate system. The resulting SSS is identical to the SSS of the worldwide model within the limits of acceptable errors, summarized in Table 4.

Table 4. Summary table of errors in the calculation of the local model.

	Displacements, mm	Average stresses, MPa	Principal stresses in OX, MPa	Principal stresses in OY, MPa
Global model	0.00171243	40.76	9.57	2.06
Local model	0.00171149	38.99	9.57	1.99
Errors, %	0.05%	4.3%	0%	3.3%

5.2 Fatigue Life Calculation

After the global-local modeling technique was worked out, the calculation of the local FEM for fatigue life was carried out, a detailed description of which is given in the previous section.

The fatigue life calculation method consists of the solver using a reference static calculation, imposing a loading sequence diagram on it. At the same time, the parameters for stopping the analysis are set in the form of the limiting loss of stiffness of the material elements. Each time this criterion is reached, the solver recalculates the static calculation to update the SSS of the material and then continues the fatigue life calculation with the updated SSS of the sample.

For the area of interest, the adhesive joint at the border of the sticky film and the surface of the sample, the number of cycles before failure, and the degradation of the material stiffness under cyclic loads were calculated. Rigidity degradation is a relative value measured in the range [0...1], where 0 is an undamaged material, and 1 is its destruction.

Figures Fig. **18** – Fig. **29** show the results of calculations for the fatigue life of the adhesive layer adjacent to the sample surface and the upper layer of the sample material along the X, Y, and XY axes.

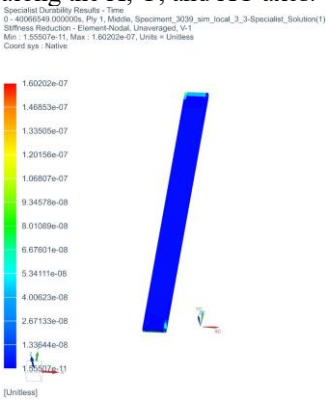

Fig. 18. Stiffness degradation of the sample material along the X axis.

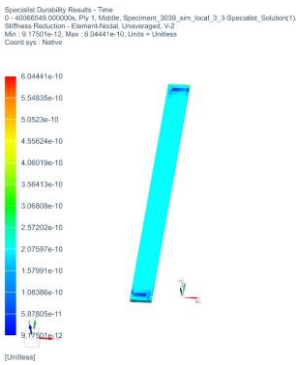

Fig. 19. Stiffness degradation of the sample material along the Y axis.

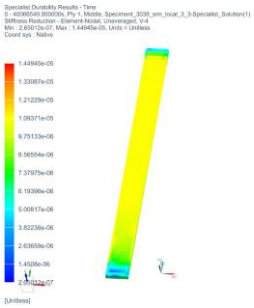

Fig. 20. Degradation of sample material stiffness along the XY axis.

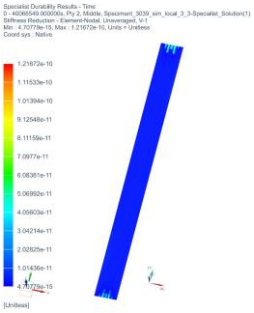

Fig. 21. Adhesive stiffness degradation along the X-axis.

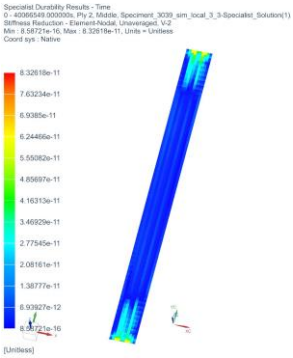

Fig. 22. Adhesive stiffness degradation along the Y-axis.

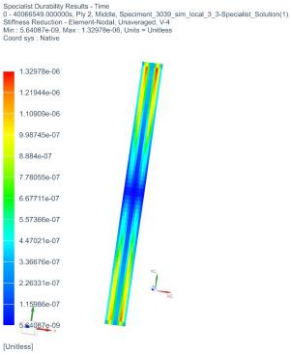

Fig. 23. Adhesive stiffness degradation along the XY-axis.

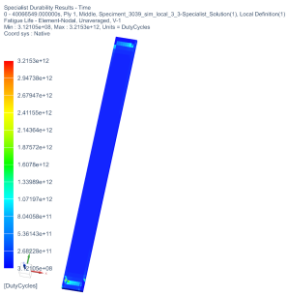

Fig. 24. Number of cycles to failure for sample material (V-1).

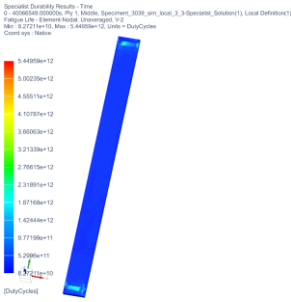

Fig. 25. Number of cycles to failure for sample material (V-2).

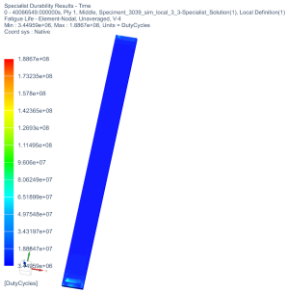

Fig. 26. Number of cycles to failure for sample material (V-4).

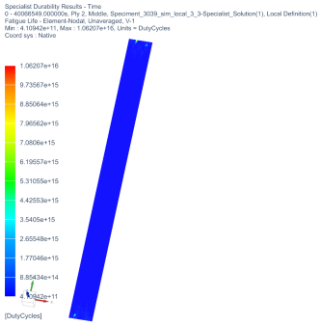

Fig. 27. Number of cycles to failure for adhesive (V-1).

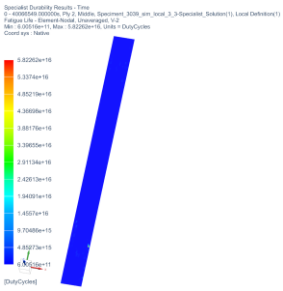

Fig. 28. Number of cycles to failure for adhesive (V-2).

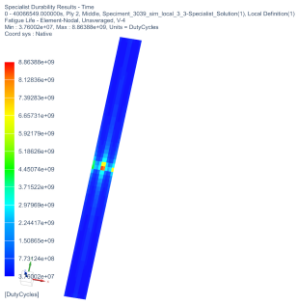

Fig. 29. Number of cycles to failure for adhesive (V-4).

6 Conclusions

Thus, within the framework of this work, a global-local modeling technique was developed, which can significantly reduce the calculation time and the required computing power. A detailed local model allows a detailed analysis of the SSS at the boundaries of the components.

According to the results of fatigue life calculations, it can be concluded that the adhesive joint with the selected characteristics satisfies the requirements of static and fatigue strength. The adhesive withstands a sufficiently large number of loading cycles and, accordingly, can be recommended for use in adhesive joints for fastening fiber-optic sensors and supply cables of the aircraft structure condition monitoring system.

Also, according to the calculations of the degradation of the adhesive joint stiffness, special attention should be paid to the initial and final sections of the gluing of the fiber-optic sensor since damage accumulates in these local zones. Therefore, in these places, the destruction of the adhesive layer or its peeling will begin, which will lead to incorrect readings of fiber-optic strain gauges.

Proceeding from these remarks, when mounting FOS on PCM products, the technology must be strictly observed - phased preparation of the gluing surface to achieve high adhesive strength between the surface and the adhesive. The durability of the adhesive joint largely depends on the mechanical characteristics of the bond, the variability of which will be considered in future studies.

References

1. M.A. Zuev, V.V. Makhsidov, M.Yu. Fedotov, A.M. Shienok, To the question of the integration of optical fiber in PCM and the measurement of material deformation using

fiber Bragg gratings, Mechanics of composite materials and structures, **20(**4), 568–574 (2014)

2. K. Steiner, R. Eduljee, X. Huang, J.G. Jr, Ultrasonic NDE techniques for the evaluation of matrix cracking in composite laminates, Compos Sci Technol., **53**, 193–198 (1995)
3. R.E. Bouazzaoui, S. Baste, G. Camus, Development of damage in a 2D woven C/SiC composite under mechanical loading: II. Ultrasonic characterization, Compos. Sci. Technol., **56(**12), 1373–1382 (1996)
4. F. A. Donaghy, D. R. Nicol, Evaluation of the Fatigue Constant n in Optical Fibers with Surface Particle Damage, J. of the American Ceramic Society, 66(8), 601–604 (1983)
5. K. M. Fadeev, D. D. Larionov, L. A. Zhikina, A. M. Minkin & D. I. Shevtsov A Fiber-Optic Sensor for Simultaneous Temperature and Pressure Measurements Based on a Fabry–Perot Interferometer and a Fiber Bragg Grating // Instruments and Experimental Techniques volume. - 2020. - №63. - С. 543-546.
6. G. Xue, X. Fang, X. Hu, L. Gong, Measurement accuracy of FBG used as a surface-bonded strain sensor installed by adhesive, Applied Optics, **57**(11), 2939 (2018)
7. Shashank Pant, Marc Genest, Lucy Li & Gang Li Structural Health Monitoring of Adhesively Bonded Skin-Stiffener Composite Joint Using Distributed Fibre Optic Sensor // European Workshop on Structural Health Monitoring. - Springer, 2022. - С. 823-830.
8. S.-C. Her, C.-Y. Huang, Effect of Coating on the Strain Transfer of Optical Fiber Sensors, Sensors, **11**(7), 6926–6941 (2011)
9. K.T. Wan, C.K.Y. Leung, N.G. Olson, Investigation of the strain transfer for surface-attached optical fiber strain sensors, Smart Materials and Structures, **17**(3), 035037 (2008)
10. B.J. Skutnik, B.D. Munsey, C.T. Brucker, Coating Adhesion Effects on Fiber Strength and Fatigue Properties, MRS Proc., **88** (1986)
11. D. Inniss, L. Shepherd, D. L. Brownlow, Q. Zhong, Influence of Polymer Coatings and Adhesion on the Mechanical Strength, Fatigue and Aging of Optical Fibers. MRS Proc., **304** (1993)